

# Chemoselective Hydrogenation of Olefins Using a Nanostructured Nickel Catalyst

Mara Klarner,<sup>[a]</sup> Sandra Bieger,<sup>[a]</sup> Markus Drechsler,<sup>[b]</sup> and Rhett Kempe<sup>\*[a]</sup>

Dedicated to Prof. Dr. Josef Breu on the occasion of his 60<sup>th</sup> birthday.

The selective hydrogenation of functionalized olefins is of great importance in the chemical and pharmaceutical industry. Here, we report on a nanostructured nickel catalyst that enables the selective hydrogenation of purely aliphatic and functionalized olefins under mild conditions. The earth-abundant metal catalyst allows the selective hydrogenation of sterically pro-

TECTED olefins and further tolerates functional groups such as carbonyls, esters, ethers and nitriles. The characterization of our catalyst revealed the formation of surface oxidized metallic nickel nanoparticles stabilized by a N-doped carbon layer on the active carbon support.

## Introduction

The selective hydrogenation of C=C double bonds is a challenging reaction and of high interest in academia and for the production of industrially relevant chemicals.<sup>[1,2]</sup> More specifically, the selective hydrogenation of olefins plays an important role in the synthesis of vitamins such as biotin and  $\beta$ -carotene.<sup>[3]</sup> Also drugs such as sertraline (anti-depressant), betamethasone (glucocorticoid), and dihydroergotamine (anti-migraine agent) are produced in this way.<sup>[4]</sup> The hydrogenation of diisobutene to isooctane is important in the petrochemical industry, because it is widely used as an anti-knock additive and as a substitute for the previously used methyl *tert*-butyl ether.<sup>[5]</sup> Furthermore, the olefin hydrogenation is used for the hardening of natural oils in the food industry for better processing and storage.<sup>[6]</sup> One possible route for olefin hydrogenation is catalytic transfer hydrogenation,<sup>[7]</sup> which is usually accompanied by the formation of easy-to-remove by-products. Most of the known and industry-relevant catalyst systems are based on the expensive noble metals ruthenium, rhodium, palladium, platinum and iridium or on difficult to handle and pyrophoric Raney nickel.<sup>[8,9]</sup> In recent years, hydrogenation with nanostructured

3d metal catalysts step into the focus for many applications as introduced by us<sup>[10]</sup> and the Beller group.<sup>[11]</sup> Also, the selective olefin hydrogenation of  $\alpha,\beta$ -unsaturated carbonyls, internal and terminal unsaturated hydrocarbons was addressed with heterogeneous iron<sup>[12]</sup>, cobalt<sup>[13]</sup> and nickel<sup>[14]</sup> catalysts. A highlight is the work of Scharnagl *et al.*<sup>[13c]</sup>, who were able to hydrogenate terminal and internal alkenes with a high tolerance of functional groups using a Co@Chitosan catalyst (2.9 mol% Co) at 60 °C and 4 MPa H<sub>2</sub> pressure or at 150 °C and 1 MPa H<sub>2</sub>, respectively. Impressively, fatty acids and sunflower oil could also be converted in high yields. Considering Ni catalysts, colloiddally stabilized Ni nanoparticles were used for the selective hydrogenation of  $\alpha,\beta$ -unsaturated carbonyl compounds at room temperature and 4 MPa H<sub>2</sub>.<sup>[14f]</sup> In addition, supported systems such as the Ni-phen@SiO<sub>2</sub> catalyst (4 mol% Ni) were developed to selectively convert substrates with different functional groups at 40 °C, 1 MPa H<sub>2</sub>.<sup>[11e]</sup> The application of flow-chemistry techniques for the selective olefin hydrogenation with nickel is particularly used in pharmaceutical manufacturing and in the synthesis of valuable biobased building blocks.<sup>[15]</sup>

Here, we report on a nanostructured nickel catalyst, which permits the selective hydrogenation of functionalized olefins. This process is chemoselective and hydrogenation-sensitive functional groups such as carbonyl compounds, esters, ethers and nitriles are well tolerated. The Ni/C catalyst is easy-to-synthesize in a two-step procedure starting from inexpensive charcoal as support material. By controlled decomposition of a Ni-salen complex precursor, catalytically active Ni nanoparticles are generated and at the same time stabilized in a nitrogen-doped carbon matrix on the support.<sup>[10d-g,11f]</sup>

## Results and Discussion

The novel Ni/C catalyst was synthesized in a practical two-step procedure according to the synthesis concept for 3d metal catalysts developed by us<sup>[10d-g]</sup> (Figure 1): Firstly, the commercially available carbon support (Norit CA1) was wet impregnated with the novel Ni-salen(prop)(di-*tert*-butyl) complex in

[a] M. Klarner, S. Bieger, Prof. Dr. R. Kempe  
Inorganic Chemistry II  
University of Bayreuth  
Universitätsstraße 30, 95440 Bayreuth (Germany)  
E-mail: kempe@uni-bayreuth.de

[b] Dr. M. Drechsler  
Bavarian Polymer Institute (BPI), KeyLab "Electron and Optical Microscopy"  
University of Bayreuth  
Universitätsstraße 30, 95440 Bayreuth (Germany)

Supporting information for this article is available on the WWW under <https://doi.org/10.1002/zaac.202100124>

© 2021 The Authors. *Zeitschrift für anorganische und allgemeine Chemie* published by Wiley-VCH GmbH. This is an open access article under the terms of the Creative Commons Attribution License, which permits use, distribution and reproduction in any medium, provided the original work is properly cited.

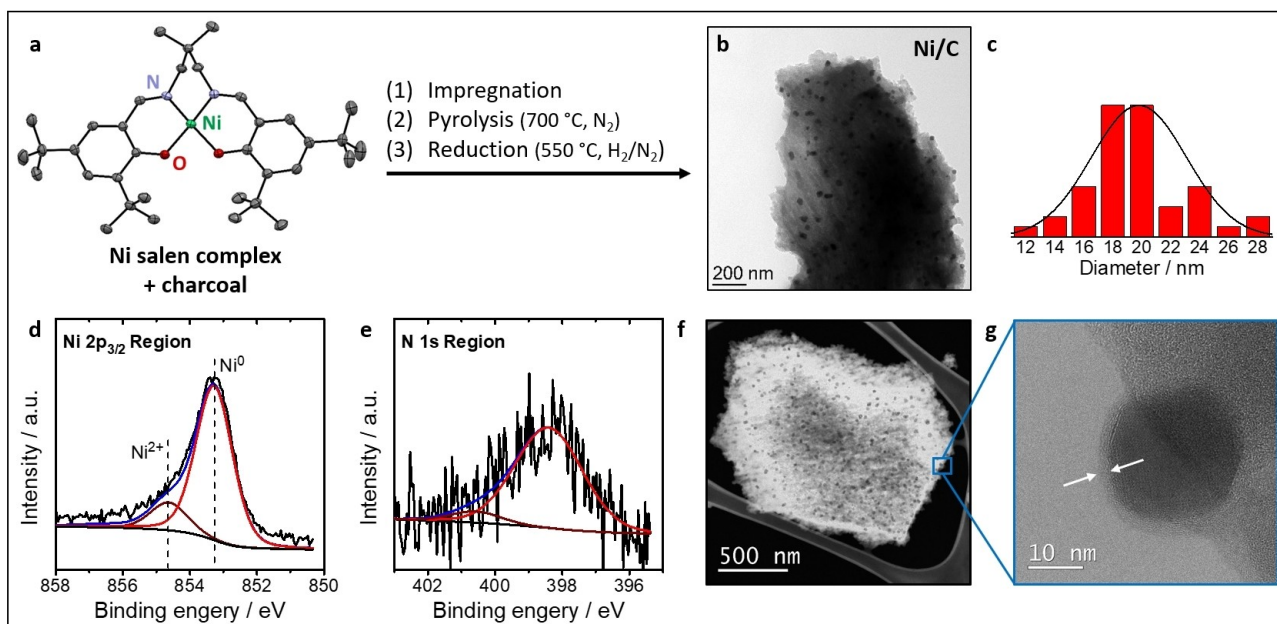


**Figure 1. Catalyst Synthesis and Characterization.** (a) Synthesis of the Ni/C catalyst by (1) wet impregnation of commercial activated charcoal (Norit CA1) with the Ni-salen(prop)(di-*tert*-butyl) complex (see Supporting Information for crystallographic data and complex characterization), followed by (2) a pyrolysis step at 700 °C in N<sub>2</sub> flow and (3) a reduction step at 550 °C in forming gas. (b, c) TEM analysis verifies the homogenous distribution of Ni nanoparticles with a mean diameter of 19.5 nm. The size distribution of Ni particles is shown as histogram. (d) XPS analysis of the Ni 2p<sub>3/2</sub> region. The Ni<sup>0</sup> nanoparticles are partially surface oxidized to Ni<sup>2+</sup> species (about 17%). (e) XPS analysis of the N 1s region. (f) Dark-field TEM analysis of the Ni/C catalyst. (g) Magnification by TEM exemplarily shows one Ni nanoparticle of 23 nm in diameter surrounded by a 2–3 nm thick carbon layer (marked with white arrows).

tetrahydrofuran and the solvent was removed (see Supporting Information for crystallographic data and complex characterization). This was followed by a pyrolysis step at 700 °C in nitrogen atmosphere and a reduction step at 550 °C in forming gas (90/10, N<sub>2</sub>/H<sub>2</sub>). We assume that the Ni catalyst is generated by molecular dispersion of a defined volatile complex compound on the support material during the pyrolysis step. The subsequent tailored decomposition of the Ni-salen complex leads to the formation of a N-doped carbon layer in which the catalytically active Ni sites are embedded. Our catalyst is very convenient to handle and remains catalytically active for several months when stored in an inert atmosphere (Supporting Information, Table S2). We performed transmission electron microscopy (TEM) and X-ray photoelectron spectroscopy (XPS) analysis to gain more insight into the catalyst structure. The catalyst consists of homogeneously distributed, spherical Ni nanoparticles with an average size of 19.5 nm and a fairly broad size distribution (Figure 1b, c). An additional dark-field TEM image verified the homogeneous distribution over the entire carbon support (Figure 1f). Detailed analysis of one Ni particle at the edge of an activated carbon platelet showed that the nanoparticle is covered by a 2–3 nm thick carbon layer (Figure 1g). This layer could only be analyzed for exposed particles, so that no average layer thickness could be determined for all supported nickel particles. Referring to our last publication, we claim that the decomposition of the Ni-salen complex leads to a N-doped carbon matrix that stabilizes the Ni particles.<sup>[10d]</sup> Elemental analysis of the catalyst material confirmed that

0.8 wt.% nitrogen from the decomposition of the Ni-salen complex remained in the Ni/C composite. To date, it is unclear to what extent the thickness and atomic composition of the N-doped carbon layer plays a key role in the catalyst activity. It is conceivable that the layer thickness and composition can be influenced by the gas flow and the choice of salen precursor during the catalyst preparation. We recorded XPS survey spectra of the Ni/C catalyst in the range of 0–1200 eV (Supporting Information, Figure S5) and observed expected lines for carbon, nickel and traces of nitrogen. In the Ni 2p<sub>3/2</sub> region (Figure 1d), the combination of a metallic Ni<sup>0</sup> signal at 852.6 eV and a broader signal at about 854.6 eV, assigned to oxidized Ni<sup>2+</sup>, was measured. The comparison of the intensity ratios at the dashed positions showed that 83% Ni<sup>0</sup> is present. Due to the handling in air, the appearance of surface-oxidized metallic Ni nanoparticles is likely. The binding energy of the N 1s signal observed is centered at 398.5 eV, possibly a remnant of the N-containing precursor molecule and its decomposition products (Figure 1e). We did not attempt to deconvolute the signal because of the low intensity. The cubic phase of metallic Ni of the freshly prepared catalyst could be indexed in the powder X-ray diffraction pattern (Supporting Information, Figure S6). This supports our thesis of surface oxidized Ni particles with metallic core. Inductively coupled plasma optical emission spectroscopy (ICP-OES) revealed a Ni content of 2.7 wt.%. This value deviates from the targeted 4 wt.% because the amount of Ni deposited on the support decreased due to the volatility of the Ni precursor during the pyrolysis process (Supporting Information,

Figure S2). Argon physisorption measurements demonstrated a 26% decrease in the surface area of the bare carbon support (929 m<sup>2</sup>/g) to 688 m<sup>2</sup>/g due to the catalyst generation process, including the particle formation (Supporting Information, Figure S7). The DFT model (Ar at 87 K on carbon, cylindrical pores) used to evaluate the pore size distribution showed an identical bimodal pore distribution for the support material and for the Ni/C catalyst. Both materials are predominantly microporous. The catalyst synthesis does not affect the absolute pore size, but only reduces the total pore volume.

We investigated the Ni/C catalyst in the hydrogenation of the C–C double bond of styrene as a catalytic benchmark test. To our delight, a low catalyst loading (1.35 mol% Ni) and very mild reaction conditions (0.2 MPa H<sub>2</sub>, 40 °C) were necessary to obtain ethylbenzene in a quantitative yield (Supporting Information, Table S2, S3). A yield of 50% was still obtained at room temperature and 0.1 MPa H<sub>2</sub> pressure, highlighting the catalytic activity of this base metal catalyst. In comparison with commercial oxidic support materials (Al<sub>2</sub>O<sub>3</sub>, CeO<sub>2</sub>, SiO<sub>2</sub>, TiO<sub>2</sub>), the combination of the Ni-salen precursor and the activated carbon support was shown to be crucial for the high catalytic activity. Remarkably, only the catalyst on silica support showed moderate catalytic activity. No hydrogenation active Ni/C catalyst could be prepared with nickel acetate as precursor, highlighting the necessity of the Ni-salen complex (Supporting Information, Table S2). Raney-Ni likewise led to quantitative yield in this benchmark reaction. With the optimized reaction conditions in hand, we were interested in the substrate scope. All given product yields were determined by gas chromatography (GC) and identified by GC-mass spectrometry (GC-MS).

Isolated yields were determined for selected examples and are given in parentheses.

Styrene (Table 1, **1 a**, 99%) and a total of 12 functionalized styrene derivatives were selectively converted to the corresponding ethylbenzene derivatives. Methyl-substituted compounds were tolerated in *para*, *meta* and *ortho* position (Table 1, **1 b** to **1 d**, 99–84%), as was the chloro-substituent (Table 1, **1 e–g**, 78–60%) with *ortho* being the most challenging position. Also, the hydrogenation of 4-bromostyrene was realized in moderate yield (Table 1, **1 h**, 50%) without dehalogenation. Electron-donating groups such as *tert*-butyl and methoxy in *para* position (Table 1, **1 i** and **1 j**) were very well tolerated by the Ni/C catalyst and the corresponding products were obtained in quantitative yields. The double bond of the N-heteroaromatic substrate 2-vinylpyridine, the 1,1-disubstituted  $\alpha$ -methoxy styrene and the polyaromatic 2-vinylnaphthalene were hydrogenated in moderate to good yields, respectively (Table 1, **1 k** to **1 m**). The hydrogenation of styrene at about 60% was chosen as the test reaction for a recyclability study. The catalyst was used in five consecutive runs and showed no reduction in activity in the first three (Supporting Information, Figure S8). Then a minor decrease in activity was observed.

Next, we investigated the transformation of purely aliphatic and aromatic unsaturated hydrocarbons. The conversion of these non-functionalized olefins required harsher reaction conditions of 80 °C and 1 MPa H<sub>2</sub>, whereas the catalyst loading did not need to be increased (Supporting Information, Table S4). 1,2-substituted C–C double bonds as in *trans*-stilbene (Table 2, **2 a**, 99%) and internally cyclic olefins such as cyclohexene, cyclooctene and norbornene were quantitatively converted to the respective saturated compounds (Table 2, **2 c** to **2 e**). In addition, terminal double bonds in vinylcyclohexane, octa-1,8-diene, 1-heptene, and 1-hexene (Table 2, **2 b** and **2 f** to

**Table 1.** Olefin hydrogenation with Ni/C: Investigation of styrene derivatives.<sup>[a]</sup>

	R = 4-Me	<b>1 b</b> , 99%
	2-Me	<b>1 d</b> , 84%
	3-Me	<b>1 c</b> , 99%
<b>1 a</b> , 99% (98%)	R = 4-Cl	<b>1 e</b> , 78%
	2-Cl	<b>1 g</b> , 60%
	3-Cl	<b>1 f</b> , 75%
	4-Br	<b>1 h</b> , 50%
		<b>1 i</b> , 99%
		<b>1 j</b> , 99%
		<b>1 k</b> , <sup>[b]</sup> 58%
		<b>1 l</b> , 84%
		<b>1 m</b> , 43%

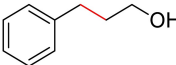
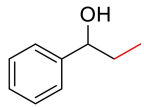
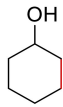
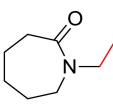
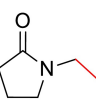
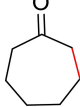
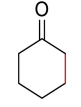
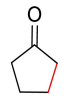
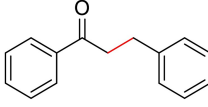
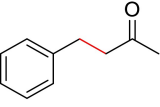
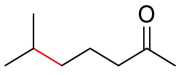
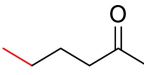
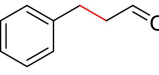
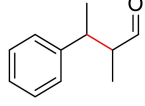
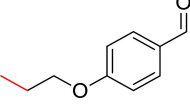
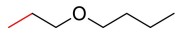
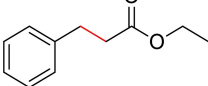
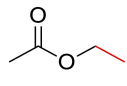
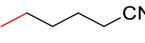
[a] 0.5 mmol substrate, 2.5 ml MeOH, 1.35 mol% Ni (14.7 mg Ni/C, 2.7 wt.% Ni), 40 °C, 0.2 MPa H<sub>2</sub>, 20 h. [b] 80 °C, 1 MPa H<sub>2</sub>. Yields determined by GC using *n*-dodecane as an internal standard. Products were analyzed by GC-MS. Isolated yields are given in parentheses.

**Table 2.** Olefin hydrogenation with Ni/C: Investigation of unsaturated hydrocarbons.<sup>[a]</sup>

<b>2 a</b> , 99% (90%)	<b>2 b</b> , 99%	<b>2 c</b> , 94%
<b>2 d</b> , 99% (99%)	<b>2 e</b> , 99%	<b>2 f</b> , 99%
<b>2 g</b> , 99%	<b>2 h</b> , 99%	<b>2 i</b> , 91%

[a] 0.5 mmol substrate, 2.5 ml MeOH, 1.35 mol% Ni (14.7 mg Ni/C, 2.7 wt.% Ni), 80 °C, 1 MPa H<sub>2</sub>, 20 h. Yields determined by GC using *n*-dodecane as an internal standard. Products were analyzed by GC-MS. Isolated yields are given in parentheses.

**Table 3.** Olefin hydrogenation with Ni/C: Investigation of functional group tolerance.<sup>[a]</sup>

 <b>3 a,</b> <sup>[b]</sup> <b>92 %</b>	 <b>3 b,</b> <sup>[b]</sup> <b>99 %</b>	 <b>3 c,</b> <sup>[b]</sup> <b>99 % (97 %)</b>	 <b>3 d,</b> <b>99 %</b>	 <b>3 e,</b> <b>99 %</b>
 <b>3 f,</b> <b>92 %</b>	 <b>3 g,</b> <b>99 % (99 %)</b>	 <b>3 h,</b> <b>99 %</b>	 <b>3 i,</b> <b>84 % (80 %)</b>	 <b>3 j,</b> <b>74 %</b>
 <b>3 k,</b> <b>84 %</b>	 <b>3 l,</b> <b>80 %</b>	 <b>3 m,</b> <b>76 %</b>	 <b>3 n,</b> <b>78 %</b>	 <b>3 o,</b> <b>99 %</b>
 <b>3 p,</b> <b>99 %</b>	 <b>3 q,</b> <b>99 %</b>	 <b>3 r,</b> <b>68 %</b>	 <b>3 s,</b> <sup>[b]</sup> <b>99 %</b>	

[a] 0.5 mmol substrate, 2.5 ml H<sub>2</sub>O, 1.35 mol% Ni (14.7 mg Ni/C, 2.7 wt.% Ni), 80 °C, 1 MPa H<sub>2</sub>, 20 h. [b] 2.5 ml MeOH. Yields determined by GC using *n*-dodecane as an internal standard. Products were analyzed by GC-MS. Isolated yields are given in parentheses.

2h) were hydrogenated in 99% yield. Furthermore, it was possible to convert a 1,1-disubstituted olefin to obtain the product 3-methylheptane in 91% (Table 2, 2i).

The application scope of the catalyst had been further extended to the olefin hydrogenation in the presence of hydrogenation-sensitive functional groups. Water was used as a solvent for C=O functionalized substrates because the methylation of carbonyl functions by the solvent methanol occurred as an undesirable side reaction. A total of 19 examples were selectively converted at 80 °C and 1 MPa H<sub>2</sub> pressure. Alcohol-modified substrates (Table 3, 3a to 3c, 92–99%) did not negatively affect the catalytic hydrogenation of C=C double bonds by Ni/C. Likewise, N-vinyl derivatives of caprolactam and pyrrolidone were quantitatively converted (Table 3, 3d and 3e) without attacking the cyclic amide. Our Ni/C catalyst enables the challenging hydrogenation of olefins in the presence of  $\alpha,\beta$ -unsaturated ketones in very good yields. Internal cyclic carbonyl compounds were converted more efficiently (Table 3, 3f to 3h, 92–99%) than non-cyclic ones (Table 3, 3i and 3j, 84% and 74%).

Furthermore, isolated mono- or trisubstituted C=C double bonds were selectively hydrogenated in the presence of keto groups (Table 3, 3k and 3l). Remarkably, hydrogenation-sensitive  $\alpha,\beta$ -unsaturated aldehydes were well tolerated. Not only a 1,2-di-substituted olefin (Table 3, 3m, 76%) but also the challenging 1,2-tetrasubstituted 2-methyl-3-phenylbutenal (Table 3, 3n, 78%) was selectively hydrogenated in good yields. Only a minor trace of alcohol was observed as a byproduct. Also, an aromatic and an aliphatic allyl ether (Table 3, 3o and

3p) and cinnamic acid ethyl ester (Table 3, 3q) were quantitatively converted to the respective saturated compounds. For unknown reasons, only a moderate yield of 68% of ethyl acetate (Table 3, 3r) could be obtained. In addition to the numerous examples of oxygen-containing functional groups, the C≡N triple bond of an aliphatic nitrile was tolerated (Table 3, 3s, 99%).

One reaction was performed with 20 times the amount of substrate (10 mmol) to demonstrate the applicability of the Ni/C catalyst on a larger scale. Styrene (95%) was converted to the corresponding saturated product with slightly reduced activity referred to the 0.5 mmol reaction.

## Conclusions

In summary, we have developed a nickel catalyst that selectively hydrogenates olefins under mild reaction conditions. The Ni/C catalyst showed a high tolerance to hydrogenation-sensitive functional groups such as carbonyl, ether, ester, and nitrile.

## Acknowledgements

This work was supported by the German Research Foundation (DFG SFB 840, B1). We thank R. Fertig for XRD, K. Ament for PXRD and F. Baier for XPS analysis. Furthermore, we thank the



Elite Network Bavaria for financial and other support. Open access funding enabled and organized by Projekt DEAL.

**Keywords:** nickel catalyst · olefins · selective hydrogenation · sustainable catalysis

- [1] H.-U. Blaser, F. Spindler, M. Thommen, J. G. De Vries, C. J. Elsevier, *The Handbook of Homogeneous Hydrogenation*, Wiley-VCH: Weinheim, **2008**.
- [2] L. A. Saudan, *Acc. Chem. Res.* **2007**, *40*, 1309.
- [3] S. Lavielle, S. Bory, B. Moreau, M. J. Luche, A. Marquet, *J. Am. Chem. Soc.* **1978**, *100*, 1558.
- [4] B. Chen, U. Dingerdissen, J. G. E. Krauter, H. G. J. Lansink Rotgerink, K. Möbus, D. J. Ostgard, P. Panster, T. H. Riermeier, S. Seebald, T. Tacke, H. Trauthwein, *Appl. Catal. A* **2005**, *280*, 17.
- [5] B. M. Goortani, A. Gaurav, A. Deshpande, F. T. T. Ng, G. L. Rempel, *Ind. Eng. Chem. Res.* **2015**, *54*, 3570.
- [6] G. List, J. W. King, *AOCs Press*. **2015**, ed. 2.
- [7] D. Wang, D. Astruc, *Chem. Rev.* **2015**, *115*, 6621.
- [8] a) M. Guerrero, N. T. Than Chau, S. Noel, A. Denicourt-Nowicki, F. Hapiot, A. Roucoux, E. Monflier, K. Philippot, *Curr. Org. Chem.* **2013**, *17*, 364; b) B. L. Albuquerque, A. Denicourt-Nowicki, C. Mériadeq, J. B. Domingos, A. Roucoux, *J. Catal.* **2016**, *340*, 144; c) M. Tamura, K. Tokonami, Y. Nakagawa, K. Tomishige, *ACS Catal.* **2016**, *6*, 3600.
- [9] a) H. Adkins, H. R. Billica, *J. Am. Chem. Soc.* **1948**, *70*, 695; b) A. F. Barrero, E. J. Alvarez-Manzaneda, R. Chahboun, R. Meneses, *Synlett*. **1999**, *10*, 1663; c) X. Ge, J. Pan, X. Chen, C. Qian, S. Zhou, *Int. J. Hydrogen Energy* **2016**, *41*, 18478.
- [10] a) G. Hahn, J.-K. Ewert, C. Denner, D. Tilgner, R. Kempe, *ChemCatChem* **2016**, *8*, 2461; b) T. Schwob, R. Kempe, *Angew. Chem. Int. Ed.* **2016**, *55*, 15175; c) C. Bäumlner, R. Kempe, *Chem. Eur. J.* **2018**, *24*, 8989; d) G. Hahn, P. Kunnas, N. de Jonge, R. Kempe, *Nat. Catal.* **2019**, *2*, 71; e) T. Schwob, P. Kunnas, N. de Jonge, C. Papp, H.-P. Steinrück, R. Kempe, *Sci. Adv.* **2019**, *5*, eaav3680; f) T. Schwob, M. Ade, R. Kempe, *ChemSusChem* **2019**, *12*, 3013; g) C. Bäumlner, C. Bauer, R. Kempe, *ChemSusChem* **2020**, *13*, 3110.
- [11] a) R. V. Jagadeesh, A.-E. Surkus, H. Junge, M.-M. Pöhl, J. Radnik, J. Rabeah, H. Huan, V. Schünemann, A. Brückner, M. Beller, *Science* **2013**, *342*, 1073; b) F. A. Westerhaus, R. V. Jagadeesh, G. Wienhöfer, M.-M. Pöhl, J. Radnik, A.-E. Surkus, J. Rabeah, K. Junge, H. Junge, M. Nielsen, A. Brückner, M. Beller, *Nat. Chem.* **2013**, *5*, 537; c) X. Cui, Y. Li, S. Bachmann, M. Scalone, A.-E. Surkus, K. Junge, C. Topf, M. Beller, *J. Am. Chem. Soc.* **2015**, *137*, 10652; d) R. Jagadeesh, K. Murugesan, A. S. Alshammari, H. Neumann, M.-M. Pohl, Marga Martina, J. Radnik, M. Beller, *Science* **2017**, *358*, 326; e) P. Ryabchuk, G. Agostini, M.-M. Pohl, H. Lund, A. Agapova, H. Junge, K. Junge, M. Beller, *Sci. Adv.* **2018**, *4*, eaat0761; f) Senthamarai, V. G. Chandrashekar, M. B. Gawande, N. V. Kalevaru, R. Zboril, P. C. J. Kamer, R. V. Jagadeesh, M. Beller, *Chem. Sci.* **2020**, *11*, 2973.
- [12] a) R. Paul, G. Hilly, *Bull. Soc. Chim.* **1939**, *6*, 218; b) A. F. Thompson, Jr., S. B. Wyatt, *J. Am. Chem. Soc.* **1940**, *62*, 2555; c) S.-i. Taira, *Bull. Chem. Soc. Jpn.* **1962**, *35*, 840; d) P.-H. Phua, L. Lefort, J. A. F. Boogers, M. Tristany, J. G. de Vries, *Chem. Commun.* **2009**, 3747; e) C. Rangheard, C. Fernández, P. Phua, J. Hoorn, L. Lefort, J. G. de Vries, *Dalton Trans.* **2010**, *39*, 8464; f) M. Stein, J. Wieland, P. Steurer, F. Tölle, R. Mülhaupt, B. Breit, *Adv. Synth. Catal.* **2011**, *353*, 523; g) R. Hudson, A. Rivière, C. M. Cirtiu, K. L. Luska, A. Moores, *Chem. Commun.* **2012**, *48*, 3360; h) V. Kelsen, B. Wendt, S. Werkmeister, K. Junge, M. Beller, B. Chaudret, *Chem. Commun.* **2013**, *49*, 3416; i) R. Hudson, G. Hamasaka, T. Osako, Y. M. A. Yamada, C.-J. Li, Y. Uozumi, A. Moores, *Green Chem.* **2013**, *15*, 2141; j) T. N. Gieshoff, M. Villa, A. Welther, M. Plois, U. Chakraborty, R. Wolf, A. Jacobi von Wangelin, *Green Chem.* **2015**, *17*, 1408; k) T. N. Gieshoff, U. Chakraborty, M. Villa, A. Jacobi von Wangelin, *Angew. Chem. Int. Ed.* **2017**, *56*, 3585.
- [13] a) B. V. Aller, *J. Appl. Chem.* **1958**, *8*, 492; b) S. U. Son, K. H. Park, Y. K. Chung, *Org. Lett.* **2002**, *4*, 3983; c) F. K. Scharnagl, M. F. Hertrich, F. Ferretti, C. Kreyenschulte, H. Lund, R. Jackstell, M. Beller, *Sci. Adv.* **2018**, *4*, eaau1248; d) S. Sandl, F. Schwarzhuber, S. Pöllath, J. Zweck, A. Jacobi v. Wangelin, *Chem. Eur. J.* **2018**, *24*, 3403; e) P. Büschelberger, E. Reyes-Rodriguez, C. Schöttle, J. Treptow, C. Feldmann, A. Jacobi von Wangelin, R. Wolf, *Catal. Sci. Technol.* **2018**, *8*, 2648; f) T. Song, Z. Ma, Y. Yang, *ChemCatChem* **2019**, *11*, 1313; g) A. Pews-Davtayan, F. K. Scharnagl, M. F. Hertrich, C. Kreyenschulte, S. Bartling, H. Lund, R. Jackstell, M. Beller, *Green Chem.* **2019**, *21*, 5104.
- [14] a) K. Hata, I. Motoyama, K. Sakai, *Org. Prep. Proced. Int.* **1972**, *4*, 179; b) D. Chatterjee, H. C. Bajaj, A. Das, K. Bhatt, *J. Mol. Catal.* **1994**, *92*, 235; c) F. Alonso, M. Yus, *Tetrahedron Lett.* **1996**, *37*, 6925; d) F. Alonso, I. Osante, M. Yus, *Synlett*. **2006**, *18*, 3017; e) V. Polshettiwar, B. Baruwati, R. S. Varma, *Green Chem.* **2009**, *11*, 127; f) M. A. Harrad, P. Valerga, M. C. Puerta, I. Houssini, M. A. Ali, L. El Firdoussi, A. Karim, *Molecules* **2011**, *16*, 367; g) V. M. Mokhov, Y. V. Popov, D. N. Nebykov, *Russ. J. Gen. Chem.* **2016**, *52*, 319; h) M. G. Prakash, R. Mahalakshmy, K. R. Krishnamurthy, B. Viswanathan, *Catal. Sci. Technol.* **2015**, *5*, 3313; i) L. Zaramello, B. L. Albuquerque, J. B. Domingos, *Dalton Trans.* **2017**, *46*, 5082; j) K. O. Sebakhly, G. Vitale, P. Pereira-Almao, *Ind. Eng. Chem. Res.* **2019**, *58*, 8597; k) J.-q. Bai, M. Tamura, Y. Nakagawa, K. Tomishige, *Chem. Commun.* **2019**, *55*, 10519; l) M. Li, J. Fu, S. Xing, L. Yang, X. Zhang, P. Lv, Z. Wang, Z. Yuan, *Appl. Catal. B* **2020**, *260*, 118114; m) T. M. Maier, S. Sandl, P. Melzl, J. Zweck, A. Jacobi v. Wangelin, R. Wolf, *Chem. Eur. J.* **2020**, *26*, 6113.
- [15] a) M. Zienkiewicz-Machnik, I. Goszewska, A. Srebrowata, A. Kubas, D. Gizinski, G. Slowik, K. Matus, D. Lisovyt'skiy, M. Pisarek, J. Sa, *Catal. Today* **2018**, *308*, 38; b) L. K. Spare, D. G. Harman, J. R. Aldrich-Wright, T. V. Nguyen, C. P. Gordon, *Adv. Synth. Catal.* **2018**, *360*, 1209; c) B. Mallesham, P. Sudarsanam, B. V. S. Reddy, B. G. Rao, B. M. Reddy, *ACS Omega* **2018**, *3*, 16839; d) B. Szabo, B. Tamas, F. Faigl, J. Eles, I. Greiner, *J. Flow Chem.* **2019**, *9*, 13; e) V. R. Madduluri, K. K. Mandari, V. Velpula, M. Varkolu, S. R. R. Kamaraju, M. Kang, *Fuel* **2020**, *261*, 116339; f) M. Kundra, T. Grall, D. Ng, Z. Xie, C. H. Hornung, *Ind. Eng. Chem. Res.* **2021**, *60*, 1989.

Manuscript received: April 9, 2021

Revised manuscript received: May 4, 2021

Accepted manuscript online: May 5, 2021